Proceedings of the 26th International Conference on
Port and Ocean Engineering under Arctic Conditions
June 14-18, 2021, Moscow, Russia

Flexural Strength of Freshwater Ice in Saimaa Area

Mikko Suominen[1], Roman Repin[1], Liangliang Lu[1], Fang Li[1], Pentti Kujala[1]
[1] Aalto University, Department of Mechanical Engineering, Espoo, Finland

ABSTRACT

Inland waterways are important for exporting goods from Eastern Finland. To develop new solutions for a sustainable and efficient transportation in these areas, INFUTURE project was launched that includes model-scale testing in Aalto Ice Tank. In order to define the ice conditions for the tests, a measurement campaign was launched that covered different areas of Saimaa and seasonal variation in 2021.

This paper presents the measurement results from the first measurement campaign on January. The measurements included flexural strength determination through cantilever beam and 3-point bending testing, strain modulus from the bending tests, ice density, and ice structure. The measured flexural strengths were 590 kPa and 780 kPa, on average, with cantilever beam and 3-point bending, respectively, giving a ratio of 1.3 between the methods. The measured strain modulus from cantilever beam and 3-point bending testing were 3.5 GPa and 3.4 GPa on average, respectively. The average density was 890 kg/m^3. Both S1 and S2 ice were encountered, where the grain size varied from 0.2 cm to 5 cm when moved from the top surface towards the bottom of the ice.

KEY WORDS: Freshwater ice; Flexural strength; Strain modulus; Structure of Ice; Three-point bending; Cantilever beam; Grain Size; Inland Waterways

INTRODUCTION

Saimaa is an important inland waterway area for Finland, as industry products are exported through waterways from different parts of Saimaa. To develop wide-ranging solutions for a sustainable and efficient inland waterway transportation, INFUTURE project was launched. As a part of the project, the most suitable vessel type for inland waterway operations is developed and designed. This includes model-scale testing in ice in Aalto Ice Tank with the design. In order to carry out model tests correctly and to ensure the scalability of the results, reliable data on actual mechanical properties of Saimaa lake ice is needed. As the ice breaking vessels are commonly designed to break ice through bending, a target flexural strength is commonly defined for the model-scale testing in ice.

Flexural strength has been tested extensively in the past with sea ice and freshwater ice (see e.g. collection by Timco and O'Brien, 1994). For sea ice, Timco and O'Brien (1994) were successful in relating the flexural strength of ice to the brine volume that is calculated from the temperature and salinity of ice. However, due to several parameters affecting the result, similar correlation has not been defined for freshwater ice (Timco and Weeks, 2010). As a brittle material and several parameters affecting the strength, the determined flexural strengths for freshwater ice have shown a great variation (Timco and O'Brien, 1994; Aly et al., 2018), where the average has ranged from 500 kPa to 2.2 MPa (Aly et al., 2018). Despite several measurement campaigns, flexural strengths are scarcely present in the literature for the Saimaa area (see John et al., 2018). Due to the great variation in the measured flexural strength of freshwater ice and lack of data from Saimaa lake ice, obtaining the flexural strength and characteristics of ice experimentally in-situ for Saimaa lake ice was considered of great importance for the project.

Thus, a measurement campaign to define the mechanical properties of ice was planned for the Saimaa area. The local operators described the local ice conditions to vary significantly depending on the strength of the local current, and the water and ice to differ in color in different locations of Saimaa due to the organic contaminants introduced to the lake through rivers falling the local lakes. Therefore, measurements in different parts of Northern and Southern Saimaa were included in the measurement campaigns. In order to cover seasonal variation, measurements were planned for January, February, and March in 2021.

This paper presents the results from the January campaign that included three locations in South, two in Northeast, and two in Northwest Saimaa areas. The testing method (cantilever vs. simple beam) was shown to have a significant impact on the determined freshwater ice flexural strength that is considered to be due to the stress concentration at the root corner of the cantilever beam (Gow, 1977; Schwartz et al., 1981; Timco and O'Brien, 1994). In order to study this, the flexural strength was determined with both methods during the January campaign and is reported in this paper. In addition, this paper presents the results from the strain modulus and density measurements, and determination of the structure of ice.

MEASUREMENT METHODS

Flexural Strength

The flexural strength was determined applying two methods, ex-situ 3-point bending, and cantilever beam testing. In a case of cantilever beam, the corners of the root were first drilled with a Covacs ice coring drill (outer diameter 16 cm). This reduced the possible stress concentration at the root. After the corners were prepared, the cantilever beam was cut with a chain saw. The ice around the beam was removed to ensure the beam does not have unwanted contact during the tests. The beam was then loaded by the actuator that had a rounded head and was instrumented with the force sensor. As the sample was at the water level, the load sensor could not reach the sample. Thus, a vertical wooden beam extension was applied between the load sensor and the sample, see Figure 1.

Figure 1. Cantilever beam test (on the left) and ex-situ 3-point bending test (on the right).

The ex-situ 3-point bending tests were conducted after each cantilever beam test. The ice beam for the 3-point bending test was cut from the tested cantilever beam sample with a chain saw and lifted to the testing rig. Cantilever and 3-point bending tests were conducted on the same samples to observe the effect of different testing methods on experimental results. It was assumed that the ice had not damaged from the middle beam during the cantilever beam testing. One of the supports of the rig was rigid while small rotation around the length of the beam was allowed by the other support. As the ice surfaces are not totally flat, this setup secured better contact at the location of supports and reduced the possible torsion during the sample loading. The loading was applied with an actuator through a force sensor at the mid span of the beam through a rounded head. This also reduced the possible torsion in the beam, see Figure 1.

In order to determine the flexural strength, the beam was assumed to behave as an Euler-Bernoulli beam. As notified e.g. by Schwartz et al. (1981), this is not actually valid for ice and the obtained values should be considered as index value. Assuming the first failure occurs on the surface in tension, i.e. the maximum normal stress in longitudinal direction defines the flexural strength, the equations for the flexural strength can be determined from equation:

$$\sigma_x = \frac{My}{I} \tag{1}$$

where σ_x [Pa] is the normal stress, M [Nm] is the bending moment affecting the cross-section, y [m] is the vertical distance from the neutral axis, and I [m^4] is the second moment of cross-sectional area. Substituting the expression for the maximal bending moment at the root of the beam in Equation (1), following form for the flexural strength from cantilever beam test ($\sigma_{Cantilever}$) can be determined:

$$\sigma_{Cantilever} = \frac{6FL_b}{bh^2} \tag{2}$$

Where F [N] is the measured force at the time of failure, L_b [m] is the length from the loading point to the location of crack, b [m] is the width of the beam, and h [m] is the height of the beam. Following the same methodology, the following form can be determined for the flexural strength in 3-point bending (σ_{3Point}):

$$\sigma_{3Point} = \frac{3x}{bh^2}\left[F + \left(L_{sup} - x\right)g\rho_i bh\right] \tag{3}$$

Where L_{sup} [m] is the length of the span, x [m] is the distance from the support to the location where the ice failed, g [m/s^2] is the acceleration due to gravity, and ρ_i [kg/m^3] is the density of ice.

Strain Modulus

Assuming the beam behaves as an Euler-Bernoulli beam, the displacement equation, $w(x)$, for the beam can be derived from the moment equation, $M(x)$, along the beam from the following relation:

$$EI\frac{d^2w}{dx^2} = -M(x) \tag{4}$$

Where E is the elastic modulus. When the change in deflection, $\Delta\delta$, is measured from a known location simultaneously with the change in force, ΔF, the strain modulus from the 3-point bending test (E_{3Point}) and cantilever beam test ($E_{Cantilever}$) can be determined with the following equations:

$$E_{3Point} = \frac{\Delta F}{\Delta \delta} \frac{3x}{bh^3} \left(\frac{L^2}{4} - \frac{x^2}{3} \right) \quad (5)$$

$$E_{Cantilever} = \frac{\Delta F}{\Delta \delta} \frac{6x^2}{bh^3} \left(L - \frac{x}{3} \right) \quad (6)$$

Where x [m] denotes the distance from the support in Equation (5) and root of the beam in Equation (6) to the location of the displacement sensor. L [m] denotes the distance between the supports in Equation (5) and the length of the cantilever beam in Equation (6).

Density of Ice

The density of ice was determined by following the ITTC Guidelines (ITTC, 2014). The density of ice is determined by submerging the ice and measuring the weight at different steps. First, lake water is poured in a bucket and the weight is recorded, w_1. An ice piece is cut from the ice sheet and placed in the water filled bucked and the second weight is recorded, w_2. As the last step, the ice sample is submerged and the third weight is recorded, w_3. The ice density can now be calculated with the following formula:

$$\frac{\rho_i}{\rho_w} = \frac{w_2 - w_1}{w_3 - w_1} \quad (7)$$

where ρ_w [kg/m^3] is the density of water, assumed to be 1000 [kg/m^3].

Structure of Ice

The ice cores that were extracted at the root of beams during the cantilever beam tests were utilized for the structure determination. After extraction of the ice samples from the ice coring drill (inner diameter 14 cm), a sample is cut horizontally into relatively thin pieces by a band saw at different depths. At least three layers from top, middle and bottom layer of the ice sample are investigated for ice structure. The locations, where the transition from one ice layer to another is clearly visible, were prioritized in the selection for horizontal sections. In addition, another ice piece is cut from the middle of the ice sample vertically, referred as vertical sections. Then, the horizontal and vertical sections are melted on a heated metal plate until thickness is around 1 mm thickness. The thin sections are then placed in-between two crossed polarizers on a light table and the grain structure of ice is observed and recorded by taking photos and videos, see Figure 2.

When the thin sections are in-between two crossed polarizers, main focuses are twofold: 1) to observe grain size change along the depth; 2) to observe collective trends in grain color change by rotating the upper polarizer in horizontal plane and with angles to 0, 45, 90 and 135 degrees to the bottom one. The latter aims to support a quick and rough judgment on the distribution of ice crystals c-axis inclination angles to categorize the type of ice. The collective statistics of c-axis inclinations in horizontal plane can be seen through observations of so-called extinction positions, i.e. polarizer rotation angles at which some of the grains appear black. Usually ice sheets composed of massive, irregularly shaped grains that come out of extinction only with an out-of-plane inclination of the upper polarizer and, hence, presumably exhibit vertical or near-vertical c-axes, are categorized to so-called Sl ice. Ice sheets composed predominantly of evenly distributed vertically-elongated crystals with scattered extinction positions at varying rotation angle and, hence, presumably exhibiting mainly horizontally oriented c-axes, are so-called S2 ice.

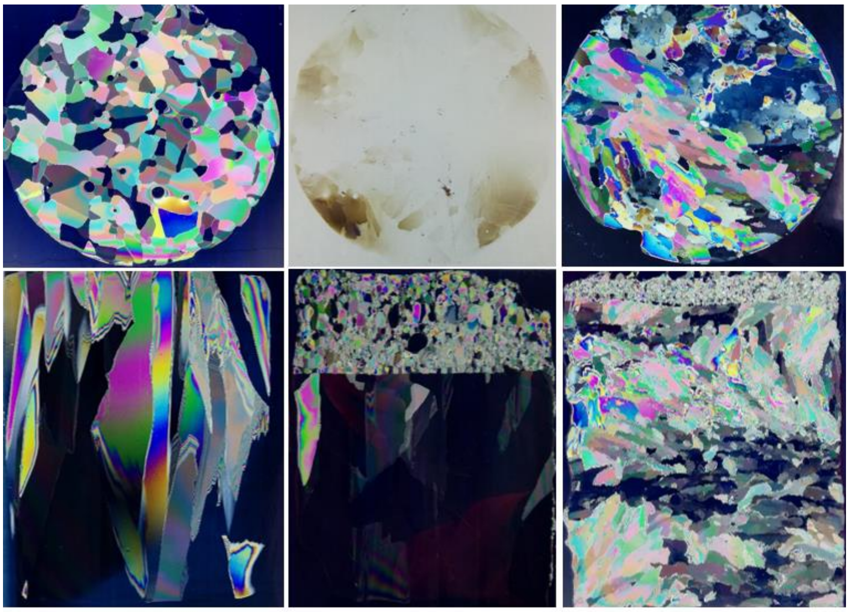

Figure 2. Three typical grain structures observed from different ice samples. C refers to the location where the sample was taken (see Table 3), H to the depth of the horizontal section (top row), and V to the depth range of the vertical section (bottom row).

MEASUREMENT LOCATIONS

General Description of Campaign

The aim of the measurements campaign was to determine the prevailing ice conditions in common operational areas in Saimaa. The possible locations were discussed with personnel of Finnpilot (a company providing the pilot services to the area) and Finnish Transport Infrastructure Agency (authority responsible of maintaining the inland waterways, among other duties). The discussions revealed that the local ice conditions vary significantly depending on the velocity of the current. The thickness may vary from half a meter of ice to open water conditions in the same area. In addition, the quality (color) was deemed different in different areas of Saimaa depending on the amount of organic material in water and ice.

Based on the discussion, locations were chosen from three different part of Saimaa: south, northeast and northwest, see Figure 3. Tiuruniemi was chosen to represent an area with a strong current effect, while Päihäniemi and Kyläniemi represent locations with minor current effect in south Saimaa where the water is clear. Vitasniemi and Vehkaniemi represent general conditions in Joensuu (northeast) area ice, where the current has minor effect, and the ice may contain organic material. Siilinjärvi represents the most difficult ice condition a ship may encounter in Saimaa area with possible organic contaminant in ice, while Puutossalmi ice describes the general conditions in Kuopio (northwest) area.

Description of Conditions in Measurement locations

Päihäniemi - January 25: The weather was calm with some wind and fog. The temperature was a few degrees below zero. The measurements were done approximately 200 m away from the shore. The samples were cut from a location that had no snow on ice. Ice thickness was 26 cm. The water and ice were clear.

Figure 3. Measurement locations. The map produced from Maanmittauslaitos Karttapaikka (Maanmittauslaitos, 2021).

Tiuruniemi - January 26: The measurements were conducted between the ship route and the shore, approximately 50 m away from the shore. The close location was chosen as the ice had visible cracks, and thickness seemed to decrease away from the shore. It was snowing the whole day and the temperature was 2.5 ^{O}C. Approximately 5 cm of slush was removed from measurement spots. Ice had negative freeboard and each cantilever beam was underwater when loaded. Ice thickness was 20 cm and transparent. Water was clear.

Kyläniemi - January 27: The location was approximately 400 m SW from Haikanniemi. Two ships were seen on the day, approximately 750 m away. The location was chosen based on the visual observation, i.e. the slush and ice surface patterns did not change. Half of the day snowed, and temperature was 1.5 ^{O}C. Approximately 5 cm of slush was removed from the testing location. Ice thickness was 14 cm and ice and water seemed transparent. Due to negative freeboard, the cantilever beams were below water when the tests were conducted.

Vitasniemi – January 29: The location was approximately 500 m away from the shore towards the shipping route. The temperature was -1.8 ^{O}C. The ice field was covered by 15-20 cm snow layer. The ice seemed to consist of two layers, a 6 cm top layer of ice formed from frozen snow and 14 cm clear bottom ice. When the cantilever beams were prepared, the beam was covered by 4 cm layer of water. The water was brownish and had clear impurities.

Vehkaniemi – January 30: Measurements were conducted halfway from shore towards the shipping route. The temperature was -2.2 ^{O}C. The ice field was covered by 25-30 cm layer of snow. The ice had a thin 1-2 cm thick snow ice layer while the total ice thickness was around 25 cm. However, the bottom had local curvatures and the thickness varied relatively significantly in short distances (~3 cm variation in thickness in 30 cm distance). This is expected to be due to currents. When the cantilever beams were prepared, the measurement site was covered by a 5 cm layer of water. No displacement measurements are available for cantilever beams. Similar to Vitasniemi, the water was brownish and had clear impurities.

Siilinjärvi – January 31: Measurements were conducted close to Yara Oy harbor, approximately 100 meters from the harbor and 10 meters from the ship channel. The temperature was -2 ^{O}C. The ice field was covered by 30 cm layer of snow. The ice consisted of several layers of ice with some brown color inclusions. Furthermore, the ice thickness and bottom shape varied significantly (from 26 cm to 37 cm) in short distances, and there were ice pieces frozen into the bottom. Possibly a result from currents, ship propeller wash, or broken ice from the channel. When the cantilever beams were prepared, the measurement site was flooded, and the ice was covered by a 3 cm layer of water. No displacement measurements are available for cantilever beams. The water seemed brown.

Puutossalmi – February 1: Measurements were conducted approximately 200 m towards south from the western point of the ferry channel. The air temperature was -9.3 ^{O}C. The ice has approximately 30 cm snow layer, and the ice thickness was 23 cm. Due to negative freeboard, the cantilever beams were tested 5 cm below the water level. Both the ice and water were clear.

RESULTS

The density was measured one to two times in each location, see Table 1 for the results. The average density was 891.5 kg/m^3. The flexural strength was determined through cantilever beam and 3-point testing each day, see Table 1. Table 1 shows that the measured flexural strength varied between the locations and the 3-point bending testing yielded 1.3 times higher flexural strenght (790 kPa, on average) than cantilever beam testing (590 kPa, on average).

The displacement measurements required for strain modulus determination were conducted when possible. Table 2 presents the average strain modulus for the cantilever beam and 3-point bending tests. The strain modules determined from cantilever beam and 3-point bending testing varied from 2.4 to 4.1 GPa and 2.6 to 5.1 GPa, respectively, giving the average of 3.5 and 3.4 GPa.

Table 1. Results from flexural strength and density measurements.

Date	Number of good tests (-)		Average flexural strength (kPa)		Average density (kg/m^3)
	Cantilever	3-point	Cantilever	3-point	
25.1.2021	1	1	527.6	842.7	885.4
26.1.2021	3	3	531.7	597.8	908.3
27.1.2021	4	4	692.9	785.3	913.9
29.1.2021	3	3	672.8	862.0	883.7
30.1.2021	2	3	490.3	811.0	912.1
31.1.2021	2	3	605.8	658.4	860.1
1.2.2021	2	1	639.1	924.0	876.8
Total / average	**17**	**18**	**594.3**	**783.0**	**891.5**

Table 2. Results from strain modulus measurements.

Date	Number of good tests (-)		Strain modulus (GPa)	
	Cantilever	3-point	Cantilever	3-point
25.1.2021	1	1	3.2	4.7
26.1.2021	3	3	4.1	2.3
27.1.2021	3	4	4.1	5.1
29.1.2021	3	3	3.7	2.9
30.1.2021	1	3	2.4	2.6
31.1.2021	0	1	na	2.7
1.2.2021	0	0	na	na
Total	**11**	**15**	**3.5**	**3.4**

Table 3 summarizes ice samples and their corresponding thin sections with grain diameter range and ice type. The grain diameter value represents the range of observed mean grain diameters averaged from horizontal top thin section layer to bottom section layer. The average grain diameter increases as a function of depth from 0.2 to 0.5 cm at the top to 1.5 to 5 cm at the bottom, see Table 3 and Figure 4. The structure analysis showed that S1 and S2 type of ice was encountered in different locations. Overall, three notable grain structures were observed. Figure 2 presents selected horizontal and vertical sections.

Table 3. Results from ice structure observations.

Date	Number of ice samples (name)	Vertical sections per sample	Horizontal sections per sample	Grain diameter range (cm)	Ice type
25.1.2021	1 (C1)	1	4	0.5-1.5	S2
26.1.2021	2 (C2-1, C2-2)	1	4	0.2-3	S2
27.1.2021	2 (C3-1, C3-2)	1	4	0.3-2	S1
29.1.2021	2 (C4-1, C4-2)	1	5 & 4	0.2-5	S1
30.1.2021	2 (C5-1, C5-2)	1	4	0.2-2.5	S2
31.1.2021	2 (C6-1, C6-2)	1	5 & 4	0.3 - 1.5	S2 + S1
1.2.2021	1 (C7)	1	4	1.5-0.8	S1 + S2

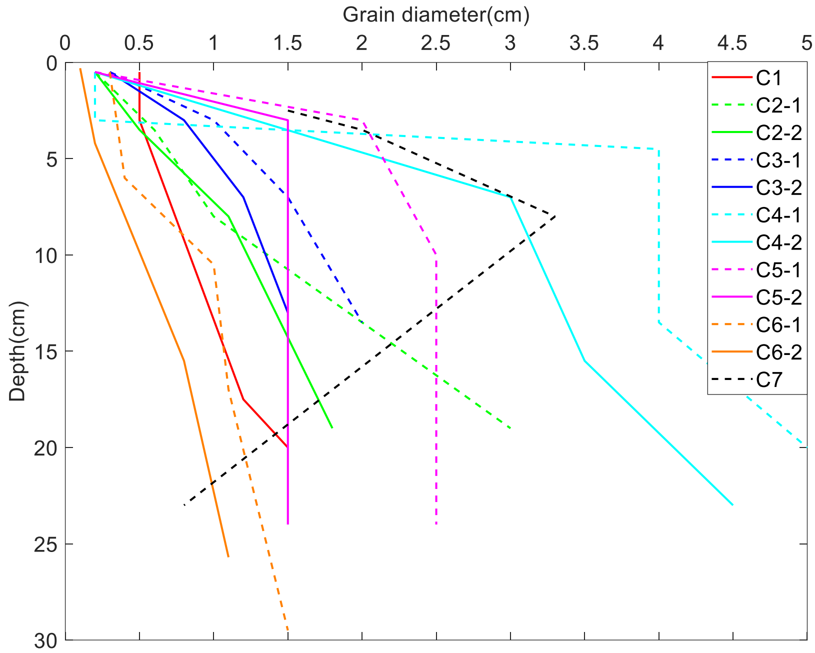

Figure 4. Measured mean grain diameters from the horizontal sections at different depths.

In samples C6-1 and C6-2, the large portion of the area of the horizontal cross sections displayed clear S2 type of structure and evenly sized grains with diameters from 4 mm to 12 mm. However, inclusions of large S1 grains (from 20 to 40 mm in size) were simultaneously observed in the same horizontal sections at the same heights of the cores and spanned over from 1/4 of the whole horizontal section area at the top up to about a half of the section area at the bottom (see Figure 5). The opposite phenomenon has been found in sample C7. Almost all horizontal sections demonstrated S1 grain structure with large grains, 20 to 50 mm in size. However, the horizontal section at the bottom core revealed about 80% of the area covered with finer S2 grains (from 4 to 11 mm in size), that showed clear change of colour upon horizontal rotation of the polarizer. The other 20% of S1 grains still present in the same horizontal section, did not demonstrate similar colour change, which facilitated the judgement on ice types (see Figure 5). The inclusion of finer S2 grains at the bottom leads to an unexpected result; the mean grain diameter for C7 sample is smaller at the bottom than at the top.

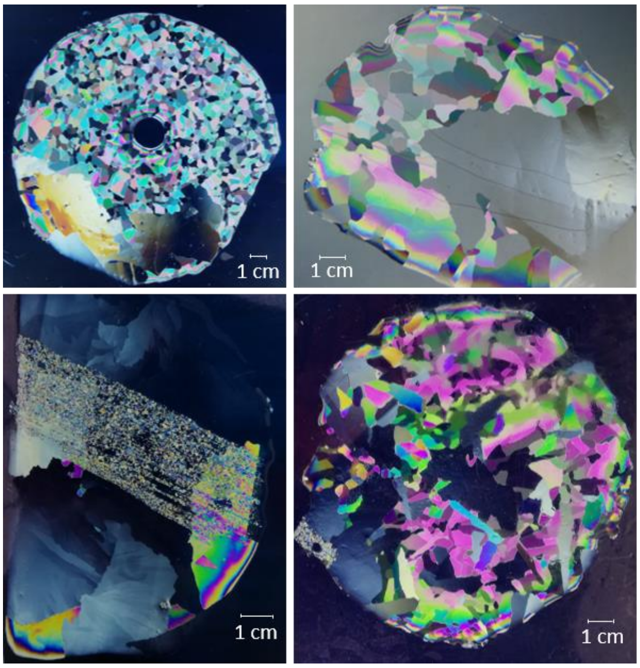

Figure 5. On the top, horizontal sections from C6-1 at a depth of 30 mm (left) and at the bottom (right). On the bottom, horizontal sections from C7 at a depth of 65 mm (left) and at the bottom (right). The stripes of very fine polygonised grains on the left are defects induced by the band saw. Large dark inclusions in the photographs are S1 grains.

DISCUSSION AND CONCLUSIONS

The paper presented the density, flexural strength, and strain modulus measurements with the determined structure of ice. The density varied from 884 to 914 kg/m^3 the average being 890 kg/m^3. The measured flexural strength was 590 kPa (on average) when tested through cantilever beam testing and 790 kPa (on average) when the 3-point bending method was applied. Thus, the 3-point bending yielded 1.3 higher flexural strength than the cantilever beam as expected. This is expected to result from the stress concentration at the root as discussed in earlier research (see e.g. Schwartz et al., 1981; Gow et al., 1988). The ratio between the values is in accordance with the earlier measurements (Gow, 1977). However, Schwartz et al. (1981) recommend testing through 4-point bending. The 4-point bending device was under construction during the 1st campaign. Thus, the testing method was not applied, but it is planned to be used in the following testing campaign.

The core or surface temperature of ice was not measured due to the lack of a proper probe. However, there is evidence in (Gow et al, 1988; Timco and O’Brien, 1994; Aly et al., 2018) that the flexural strength of freshwater ice is not affected by the ice temperature. Therefore, the absence of temperature readings is considered only a minor downside for applicability of the experimental results. Nevertheless, temperature measurements are included in February and March campaigns.

The strain modulus determined through the cantilever beam and 3-point bending testing yielded values of 3.5 and 3.4 GPa on average, respectively. As the measurements did not show any clear pattern that one method would result in a higher value, it appears the testing method does not affect the obtained values. This is in line with the extensive laboratory experiments by Gow et al. (1988).

The structure of ice (grain size and type of ice) was determined from thin sections. The observed grain size varied from 0.2 cm at the top to 5 cm at the bottom of ice. In addition, both S1 and S2 type of ice were observed. These observations and measurements were obtained through visual observation. The aim of the measurement was to obtain a preliminary understanding of the structure and type of the tested ice in the field. Samples were collected from each measurement location and preserved in a freezer. More thorough analysis shall be conducted as a future work in a laboratory with an universal Rigsby stage.

ACKNOWLEDGEMENTS

Authors would like to thank the personnel of Finnpilot and Finnish Transport Infrastructure Agency (FTIA) for the help in identifying the locations for the measurements. Special thanks to Sami Saarinen (Finnpilot), for organizing the meeting and communication with Saimaa pilots, Saimaa pilots, and Jukka Väisänen (FTIA), for suggesting and commenting on the locations for the measurements. Authors would also like to thank Eetu Pajarinen (Oy Saimaa Terminals Ab) and Marko Räisänen (Jomatrix Oy) for practical help in organizing measurements. This work has also received support from the South-eastern Finland–Russia CBC 2014–2020 program via the project Future Potential of Inland Waterways (INFUTURE).

REFERENCES

Aly, M., Taylor, R., Bailey Dudley, E., Turnbull, I., 2018. Scale effect in freshwater ice flexural strength. In: *Proceedings of the ASME 2018 37th OMAE Conference*.

Gow, A.J., 1977. Flexural strength of ice on temperate lakes. *Journal of Glaciology*, 19(81), pp. 247-256.

Gow, A.J., Ueda, H.T., Govoni, J.W., Kalafut, J., 1988. *Temperature and structure dependence of the flexural strength and modulus of freshwater model ice*, Hanover, New Hampshire, USA: CRREL Report 88-6.

John, M., Suominen, M., Sormunen, O.-V., Hasan, M., Kurvinen, E., Kujala, P., Mikkola, A., Louhi-Kultanen, M., 2018. Purity and mechanical strength of naturally frozen ice in wastewater basins. *Water Research*, 145, pp. 418-428.

International Towing Tank Conference (ITTC) 2014. *7.5-02-04-2 Test Methods for Model Ice Properties*.

Maanmittauslaitos - Karttapaikka, 2021. Online mapping service Karttapaikka [online] Available at: https://asiointi.maanmittauslaitos.fi/karttapaikka/ (Accessed March 4, 2021)

Schwartz, J., Frederking, R., Gavrillo, V., Petrov, I.G., Hirayama, K.-I., Mellor, M., Tryde, P., Vaudrey, K.D., 1981. Standardized Testing Methods for Measuring Mechanical Properties of Ice. *Cold Regions Science and Technology*, 4, pp. 245–253.

Timco, G.W., O'Brien, S., 1994. Flexural strength equation for sea ice. *Cold Regions Science and Technology*, 22, pp. 285–298.

Timco, G.W., Weeks, W.F., 2010. A review of the engineering properties of sea ice. *Cold Regions Science and Technology*, 60, pp. 107–129.